MDPI

Article

Global Stability Analysis of the Model of Series/Parallel Connected CSTRs with Flow Exchange Subject to Persistent Perturbation on the Input Concentration

Alejandro Rincón [1,2], Fredy E. Hoyos [3,*] and John E. Candelo-Becerra [4]

[1] Grupo de Investigación en Desarrollos Tecnológicos y Ambientales—GIDTA, Facultad de Ingeniería y Arquitectura, Universidad Católica de Manizales, Carrera 23 N. 60-63, Manizales 170002, Colombia; arincons@ucm.edu.co

[2] Grupo de Investigación en Microbiología y Biotecnología Agroindustrial—GIMIBAG, Instituto de Investigación en Microbiología y Biotecnología Agroindustrial, Universidad Católica de Manizales, Carrera 23 N. 60-63, Manizales 170002, Colombia

[3] Facultad de Ciencias, Escuela de Física, Universidad Nacional de Colombia–Sede Medellín, Carrera 65 No. 59A, 110, Medellín 050034, Colombia

[4] Departamento de Energía Eléctrica y Automática, Facultad de Minas, Campus Robledo, Universidad Nacional de Colombia–Sede Medellín, Carrera 80 No. 65–223, Medellín 050041, Colombia; jecandelob@unal.edu.co

[*] Correspondence: fehoyosve@unal.edu.co; Tel.: +57-(6)-8933050; Fax: +57-(6)-8782937

Abstract: In this paper, we study the convergence properties of a network model comprising three continuously stirred tank reactors (CSTRs) with the following features: (i) the first and second CSTRs are connected in series, whereas the second and third CSTRs are connected in parallel with flow exchange; (ii) the pollutant concentration in the inflow to the first CSTR is time varying but bounded; (iii) the states converge to a compact set instead of an equilibrium point, due to the time varying inflow concentration. The practical applicability of the arrangement of CSTRs is to provide a simpler model of pollution removal from wastewater treatment via constructed wetlands, generating a satisfactory description of experimental pollution values with a satisfactory transport dead time. We determine the bounds of the convergence regions, considering these features, and also: (i) we prove the asymptotic convergence of the states; (ii) we determine the effect of the presence of the side tank (third tank) on the transient value of all the system states, and we prove that it has no effect on the convergence regions; (iii) we determine the invariance of the convergence regions. The stability analysis is based on dead zone Lyapunov functions, and comprises: (i) definition of the dead zone quadratic form for each state, and determination of its properties; (ii) determination of the time derivatives of the quadratic forms and its properties. Finally, we illustrate the results obtained by simulation, showing the asymptotic convergence to the compact set.

Keywords: global attractive set; Lyapunov stability; global asymptotic stability; invariance; diffuse flow modelling

1. Introduction

Several systems converge to a compact set instead of an equilibrium point, for instance: (i) chaotic systems [1–3]; (ii) closed-loop systems subject to external disturbances or model uncertainties [4–7], or input saturation [8–10]. For this type of system, the global stability analysis considers large but bounded initial values of the state variables, and comprises determining the convergence region of the state variables, proving asymptotic or exponential global stability, and proving the invariance of the convergence region [2,3]. To this end, the Lyapunov function can be used, which consists of a radially unbounded function, possibly a quadratic form.

There are three common approaches based on the Lyapunov function for studying the aforementioned systems converging to compact sets. In the first approach, the Lyapunov

function is positive definite, and can include quadratic forms of states with some deviation. The expression of the time derivative of the Lyapunov function is arranged as a first order differential equation, and it is concluded that the Lyapunov function converges exponentially to a compact set [2,3,11]. As an example, in Zhang (2017), the stability of a Lorenz system is determined for three different ranges of a model parameter [3]. This system consists of three ordinary differential equations (ODEs). In Liao (2017), the stability of a Yang-Chen system is analyzed [2]. The system consists of three ODE's with states x, y, z. Global stability of both compact sets and equilibrium points are studied. To study global exponential convergence to compact sets, different radially unbounded Lyapunov functions are constructed for different quadrant regions of the state plane. Also, the ranges of a model parameter that imply global stability or instability of the equilibrium points are determined.

In the second approach, the Lyapunov function is positive definite and the expression of the time derivative of the Lyapunov function is negative when the state variables are outside the convergence region. It is concluded that the system converges asymptotically [3,11].

The third approach comprises dead-zone radially unbounded positive functions. This approach has been traditionally used for robust control design, but not for open-loop systems. An early development is presented in [12–14], and further developments in [15–17]. The main advantages of this approach are: (i) it allows rigorous proof of the asymptotic convergence to compact sets, through Barbalat's lemma; (ii) it facilitates stability analysis for the case that asymptotic but not exponential convergence occurs [16–18]. In Rincon (2020), this approach was used to determine the convergence of a continuously stirred tank reactor (CSTR) open-loop system that comprises three reactions in the presence of an external disturbance [19]. This system is described by three cascaded differential equations whose states converge to a compact set. In the particular case of bioreaction systems, there are several global stability studies, proving convergence to equilibrium points, but not the convergence to compact set [20–22].

Another result of global stability analysis for systems converging to compact sets is BIBO stability. It can be performed for the case of bounded or L_2 disturbances, and it results in an input–output relationship that relates the system output or states in terms of either the input signal or the time integral of the squared input signal, where the input signal may be an external disturbance or a manipulated input. This expression is obtained by integrating the time derivative of the Lyapunov function. A BIBO stability study for an open loop system is presented in [23], where a non-linear Caputo fractional system with time varying bounded delay is considered. A quadratic Lyapunov function is defined, and the resulting fractional derivative is a function of the negative Lyapunov function. As a consequence of this expression, the upper bound of the Lyapunov function, system states and system output are a function of the upper bound of the input.

BIBO stability is also determined for closed loop systems (see [24–28]). In [24], a semi-active controller is formulated for a vibrating structure. The Lyapunov analysis is combined with passivity theory and uses a storage function as a Lyapunov function. The BIBO stability result relates the displacements and velocities as a function of L_2 external forces. Also, the ranges of the controller parameters that lead to BIBO stability are defined. In [25], a robust observer-based controller design is formulated for a class of nonlinear systems described by Tagaki–Sugeno (TS) models, subject to persistent bounded external disturbance. A non-quadratic Lyapunov function is used. The BIBO stability result relates the closed loop states as a function of the external disturbance. In [26], an adaptive neural controller is developed for a n-link rigid robotic manipulator. Neural networks are used for approximating the unknown dynamics, and the backstepping strategy is used as a basic control framework. As a result of the controller design, the overall Lyapunov function (V_2) comprises the subsystem Lyapunov functions associated to the z_i states and the parameter updating error. The dV_2/dt expression is a function of V_2, so that it is concluded that the zi states converge to compact sets whose width depends on the neural approximation error.

In this paper, we study the stability of a network model comprising three CSTRs with the following features: (i) the pollutant concentration in the inflow to the first CSTR is time varying; (ii) the first and second CSTRs are connected in series, whereas the second and third CSTRs are connected in parallel with flow exchange; (iii) the states converge to a compact set instead of an equilibrium point. The practical applicability of the arrangement of CSTRs is to provide a simpler model of pollution removal from wastewater treatment via constructed wetlands, generating a satisfactory description of experimental pollution values with a satisfactory transport dead time. The aforementioned features make the global stability analysis complex. The convergence sets of the system states are determined as a function of the concentration of the inflow to the first tank, and the global asymptotic convergence of the states to these sets and their invariant nature are proved. Also, the effect of the presence of flow exchange on the transient value of the system states is determined, and it is concluded that it has no effect on the convergence regions. The study is based on global stability using dead zone Lyapunov functions and Barbalat's lemma.

The contribution of this work with respect to closely related studies on global stability of continuous stirred tank reactors (CSTR) are:

- we consider three connected CSTRs, including a side CSTR with flow exchange, whereas related studies consider a single CSTR with several states (e.g., biomass and substrate concentrations) [20,21,29,30];
- we consider the case that the system converges to a compact set, whereas related studies consider convergence to an equilibrium point [20,21,29,30].

The paper is organized as follows. The preliminaries and description of the model are presented in Section 2; the stability analysis is presented in Section 3, including the first tank (Section 3.1) and both the second and third tanks (Section 3.2). The numerical simulation is presented in Section 4, and the conclusions in Section 5.

2. Model Description

Modelling of constructed wetlands is complex because of the large number of processes involved in pollution removal, the hydraulics in a porous medium with the diffusive flow, and the dead time. In addition, the pollution removal is influenced considerably by the hydraulics and environmental conditions. The last generation of models (process—based models) are rigorous but overly complex, with difficult estimation of its parameters [31–33]. In contrast, series/parallel connection of CSTRs is simple and capable of describing transport dead time, diffusion and reaction [31].

In Marsili (2005), a simple model is proposed for describing the disperse hydraulics and pollution removal dynamics in horizontal subsurface constructed wetlands [31]. The structure of the hydraulic model comprises three series CSTRs, followed by two parallel CSTRs, and a plug flow reactor. The parallel CSTRs involve no flow exchange. The kinetics is of the Monod type, and only depends on the concentration of the modelled pollutant. The outlet and inlet flows of the system are the same, and the liquid CSTR volumes are constant. The model was fitted to both experimental tracer data and current (no tracer) data.

In Davies (2007) and Freire (2009), a simple modelling strategy is proposed for describing hydraulics and pollution removal dynamics corresponding to tracer data from vertical subsurface constructed wetlands [34,35]. The model comprises three CSTRs, the first and second CSTRs are connected in series, whereas the second and third CSTRs are connected in parallel with flow exchange. The inlet flow is considered different from the outlet flow, and no model is considered for it. The liquid volumes of the parallel CSTRs are constant, whereas the liquid volume of the first CSTR is considered varying and is described by a first-order differential equation that is fitted to experimental data. The specific reaction rate is of the first order and it only depends on the concentration of the modelled pollutant.

We use the global stability definition as follows.

Definition 1. *Consider the system dX/dt = f(X), where $X = (x_1, x_2, \ldots, x_n) \in \mathcal{R}^n, f\colon \mathcal{R}^n \to \mathcal{R}^n$, $X(t,t_0,X_o)$ denoted as X(t) is a solution to the system, and $X_0 \in \mathcal{R}^n$ is an initial value of X(t). Consider the compact set $\Omega_Q \subset \mathcal{R}^n$. Define the distance between the solution X and the compact set Ω_Q as:*

$$\rho\left(X, \Omega_Q\right) = \inf_{Y \in \Omega_Q} ||X - Y||.$$

If for all X_0 satisfying $X_0 \in \mathcal{R}^n$, $X_0 \notin \Omega_Q$ the property $\lim_{t \to \infty} \rho\left(X, \Omega_Q\right) = 0$ holds, then the compact set Ω_Q is called a global convergence set of the system, and the system is called globally asymptotically stable.

We consider a series/parallel CSTRs-based model for representing the hydraulics and pollution removal dynamics in subsurface constructed wetlands, resulting from a combination of the models proposed by [31,34]. A single pollutant and a time-varying inflow pollutant concentration are considered. The CSTRs connection comprises three CSTRs, the first and second CSTRs are connected in series, whereas the second and third CSTRs are connected in parallel with flow exchange (Figure 1). The mass balances for the CSTRs are:

$$\frac{dS_1}{dt} = (S_{in} - S_1)\frac{Q}{v_1} - r_{s1}, \tag{1}$$

$$\frac{dS_2}{dt} = (S_1 - S_2)\frac{Q}{v_2} - r_{s2} + \frac{Q_D}{v_2}(S_3 - S_2), \tag{2}$$

$$\frac{dS_3}{dt} = (S_2 - S_3)\frac{Q_D}{v_3}, \tag{3}$$

$$S_{in} = \overline{S}_{in} + \delta_{sin}, \tag{4}$$

where S_1 is the pollutant concentration in CSTR 1; S_2 is the pollutant concentration in CSTR 2; S_3 is the pollutant concentration in CSTR 3; S_{in} is the inlet pollutant concentration; Q is the wastewater flow entering CSTR 1 and CSTR 2; Q_D is the wastewater flow entering and leaving CSTR 3; v_i is the liquid volume of the ith CSTR; r_{s1} is the reaction rate of CSTR 1; r_{s2} is the reaction rate of CSTR 2. In addition, S_1 is defined in $\mathbb{R}^+$, S_2 is defined in $\mathbb{R}^+$, S_3 is defined in $\mathbb{R}^+$.
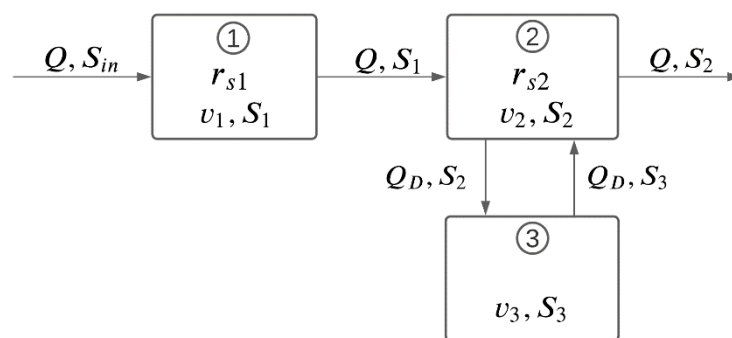
Figure 1. Schematic structure of the series/parallel continuously stirred tank reactor (CSTR)-based model.

Assumptions:

Assumption 1. *Q, Q_D, v_1, v_2, and v_3 are positive and constant. This implies that Q/v_1, Q/v_2, Q_D/v_2 and Q_D/v_3 are constant and positive.*

Assumption 2. *$\overline{S}_{in}$ is positive and constant, δ_{sin} is varying but bounded, $max\{\delta_{sin}\} > 0$, $min\{\delta_{sin}\} < 0$.*

Assumption 3. *The reaction rate r_{s1} only depends on S_1, it is bounded for S_1 bounded, $\frac{dr_{s1}}{dS_1} \geq 0$; r_{s2} only depends on S_2, it is bounded for S_2 bounded, and $\frac{dr_{s2}}{dS_2} \geq 0$.*

In the case of constant S_{in}, $\delta_{sin} = 0$ in Equation (4), S_1 converges to S_1^{eq}, S_2 converges to S_2^{eq} and S_3 converges to S_3^{eq}, where S_1^{eq}, S_2^{eq} and S_3^{eq} are positive constants obtained by equating Equations (1)–(3) to zero:

$$0 = (\bar{S}_{in} - S_1)\frac{Q}{v_1} - r_{s1}, \tag{5}$$

$$0 = (S_1 - S_2)\frac{Q}{v_2} - r_{s2} + \frac{Q_D}{v_2}(S_3 - S_2), \tag{6}$$

$$0 = (S_2 - S_3)\frac{Q_D}{v_3}. \tag{7}$$

Let

$$x_1 = S_1 - S_1^{eq}, \tag{8}$$

$$x_2 = S_2 - S_2^{eq}, \tag{9}$$

$$x_3 = S_3 - S_3^{eq}. \tag{10}$$

The x_1 dynamics is obtained by subtracting Equation (5) from Equation (1):

$$\frac{dx_1}{dt} = -D\left(x_1 + \frac{r_{x1}}{D} - \delta_{sin}\right), \tag{11}$$

$$r_{x1} = r_{s1} - r_{s1}^{eq}, \tag{12}$$

where $D = Q/v_1 > 0$, r_{s1}^{eq} is r_{s1} evaluated at $S_1 = S_1^{eq}$.

The x_2 dynamics is obtained by subtracting Equation (6) from Equation (2):

$$\frac{dx_2}{dt} = (x_1 - x_2)\frac{Q}{v_2} - r_{x2} - \frac{Q_D}{v_2}(x_2 - x_3), \tag{13}$$

$$r_{x2} = r_{s2} - r_{s2}^{eq}. \tag{14}$$

The term r_{s2}^{eq} is r_{s2} evaluated at $S_2 = S_2^{eq}$.

The x_3 dynamics is obtained by subtracting Equation (7) from Equation (3):

$$\frac{dx_3}{dt} = (x_2 - x_3)\frac{Q_D}{v_3}. \tag{15}$$

In addition, x_1 is defined in $[-S_1^{eq}, \infty)$, x_2 is defined in $[-S_2^{eq}, \infty)$, and x_3 is defined in $[-S_3^{eq}, \infty)$. The model is fitted to current (no tracer) data in Section 3.

3. Global Stability Analysis

In this section, the stability analysis is performed for the network model (1), including the determination of the convergence set, the asymptotic convergence and the invariance. The stability analysis is based on Lyapunov theory and Barbalat's lemma. Recall that early global stability studies based on dead zone Lyapunov functions are presented in [12–14], whereas later studies are presented in [16,17,19].

A dead zone quadratic form V_1 is defined for the first state x_1, V_2 for the second state x_2 and V_3 for the third state x_3, and their properties are determined. An overall Lyapunov function V is defined as a weighted sum of the quadratic forms V_1, V_2, and V_3. The time derivative of each dead zone quadratic form is determined. The stability analysis of the first tank is independent of the other tanks, whereas the stability analysis of the second and third tanks is simultaneous and requires the stability results of the first tank.

3.1. Stability Analysis for the First Tank

The stability analysis is based on determining the non-positive nature of dV_1/dt, where V_1 is the dead-zone quadratic form for x_1. The function V_1 and its gradient dV_1/dx_1 are defined so as to achieve this goal.

The procedure comprises the following tasks: (i) determination of the expression for dV_1/dt; (ii) definition of the gradient dV_1/dx_1 and the dead zone quadratic form V_1 for the state x_1; (iii) arrangement of the dV_1/dt expression in terms of a non-positive function of dV_1/dx_1; (iv) integration of the dV_1/dt expression. The definition of the gradient dV_1/dx_1. and V_1 requires the determination of the dV_1/dt expression and the properties of the terms involved.

Theorem 1. *Consider the model in Equations (11) and (12), subject to assumptions 1 to 3. (Ti) The state x_1 converges asymptotically to Ω_{x1}, $\Omega_{x1} = \left\{ x_1 : x_1^l \leq x_1 \leq x_1^u \right\}$, where $x_1^u = \{ x_1 : g_{x1} - max\{\delta_{sin}\} = 0 \}$, $x_1^u > 0$, $x_1^l = \{ x_1 : g_{x1} - min\{\delta_{sin}\} = 0 \}$, $x_1^l < 0$, and $g_{x1} = x_1 + \frac{r_{x1}}{D}$, and S_1 converges asymptotically to Ω_{S1} where $\Omega_{S1} = \left[S_1^l \ \ S_1^u \right]$, $S_1^l = x_1^l + S_1^{eq}$, $S_1^u = x_1^u + S_1^{eq}$ and S_1^{eq} is provided by Equation (5). (Tii) The sets Ω_{x1} and Ω_{S1} are invariant.*

Proof. Task 1. Determination of the dV_1/dt expression.

The time derivative of V_1 can be expressed as:

$$\frac{dV_1}{dt} = f_{v1} \frac{dx_1}{dt}, \tag{16}$$

$$f_{v1} = \frac{dv_1}{dx_1}. \tag{17}$$

Incorporating the x_1 dynamics (11) and arranging, yields:

$$\frac{dV_1}{dt} = (-1)Df_{v1}(g_{x1} - \delta_{sin}), \tag{18}$$

where,

$$g_{x1} = x_1 + \frac{r_{x1}}{D}, \tag{19}$$

$$\frac{dg_{x1}}{dx_1} = 1 + \frac{1}{D}\frac{dr_{x1}}{dx_1} \geq 1. \tag{20}$$

□

Task 2. Definition of the gradient dV_1/dx_1 and the dead zone quadratic form V_1 for the state x_1.

At what follows, we examine the properties of the term $g_{x1} - \delta_{sin}$ appearing in Equation (18). From Equations (12), (19) and (20) and Assumption 3 we have:

$$\frac{dg_{x1}}{dx_1} \geq 1; \ g_{x1} = 0 \ for \ x_1 = 0; \ sgn(g_{x1}) = sgn(x_1), \tag{21}$$

$$g_{x1} - \delta_{sin} > 0 \quad for \ x_1 > x_1^u, \tag{22}$$

$$g_{x1} - \delta_{sin} < 0 \quad for \ x_1 < x_1^l, \tag{23}$$

where,

$$x_1^u = \{ x_1 : g_{x1} - max\{\delta_{sin}\} = 0 \}, x_1^u > 0, \tag{24}$$

$$x_1^l = \{ x_1 : g_{x1} - min\{\delta_{sin}\} = 0 \}, \ x_1^l < 0. \tag{25}$$

Therefore,

$$sgn(g_{x1} - \delta_{sin}) = sgn(x_1) = sgn(g_{x1}) \ for \ x_1 \notin \left[x_1^l, x_1^u \right]. \tag{26}$$

To obtain non-positive dV_1/dt in Equation (18), we need to choose f_{v1} such that:

$$-f_{v1}(g_{x1} - \delta_{sin}) < 0 \quad for \ x_1 \notin \left[x_1^l, x_1^u\right], \tag{27}$$

$$-f_{v1}(g_{x1} - \delta_{sin}) = 0 \quad for \ x_1 \notin \left[x_1^l, x_1^u\right]. \tag{28}$$

In view of properties (26) and to fulfill conditions (27) and (28), we choose:

$$f_{v1} = \begin{cases} x_1 - x_1^u \ for \ x_1 > x_1^u \\ 0 \ for \ x_1 \ \in \ \left[x_1^l, x_1^u\right]. \\ x_1 - x_1^l \ for \ x_1 < x_1^l \end{cases} \tag{29}$$

The main properties of f_{v1} are:

$$(Pi) f_{v1} \ is \ continuous \ with \ respect \ to \ x_1 \ , \tag{30}$$

$$(Pii) \ f_{v1} = 0 \ for \ x_1 \ \in \ \left[x_1^l, x_1^u\right], \tag{31}$$

$$(Piii) \ f_{v1} \neq 0 \ for \ x_1 \ \notin \ \left[x_1^l, x_1^u\right], \tag{32}$$

$$P(iv) \ sgn(f_{v1}) = sgn(x_1) \neq 0 \ for \ x_1 \ \notin \ \left[x_1^l, x_1^u\right], \tag{33}$$

$$(Pv) \ sgn(f_{v1}) = sgn(g_{x1}) = sgn(g_{x1} - \delta_{sin}) \neq 0 \ for \ x_1 \ \notin \ \left[x_1^l, x_1^u\right]. \tag{34}$$

A dead-zone Lyapunov function that satisfies $dV_1/dx_1 = f_{v1}$ (Equation (17)) is:

$$V_1 = \frac{1}{2}f_{v1}^2. \tag{35}$$

The main properties of V_1 are:

$$V_1 > 0 \ for \ x_1 \ \notin \ \left[x_1^l, x_1^u\right], \tag{36}$$

$$V_1 = 0 \ for \ x_1 \in \ \left[x_1^l, x_1^u\right]. \tag{37}$$

$\square$

Task 3. Arrangement of the dV_1/dt expression in terms of a non-positive function of $f_{v1} = dV_1/dx_1$.

From properties (31), (34), it follows that the term $f_{v1}(g_{x1} - \delta_{sin})$ appearing in Equation (18) satisfies:

$$f_{v1}(g_{x1} - \delta_{sin}) = |f_{v1}||(g_{x1} - \delta_{sin})| \geq 0. \tag{38}$$

From the definition of g_{x1} (19) and definitions of x_1^l, x_1^u (24), (25), it follows that:

$$\lfloor g_{x1} - \delta_{sin} \rfloor \geq |g_{t1}|, \tag{39}$$

$$g_{t1} = \begin{cases} g_{x1} - max\{\delta_{sin}\} \ for \ x_1 > x_1^u \\ 0 \ for \ x_1 \in \ \left[x_1^l, \ x_1^u\right] \\ g_{x1} - min\{\delta_{sin}\} \ for \ x_1 < x_1^l \end{cases} . \tag{40}$$

From Equations (38) and (39), it follows that:

$$f_{v1}(g_{x1} - \delta_{sin}) \geq |f_{v1}||g_{t1}| = f_{v1}g_{t1} \geq 0. \tag{41}$$

From the property (21), definition of g_{t1} (40), and definition of f_{v1} (29), it follows that:

$$|g_{t1}| \geq |f_{v1}|. \tag{42}$$

Therefore, Equation (41) yields:

$$f_{v1}(g_{x1} - \delta_{sin}) \geq f_{v1}^2 \geq 0. \tag{43}$$

Using this in Equation (18) yields:

$$\frac{dV_1}{dt} \leq -Df_{v1}^2. \tag{44}$$

Accounting for the definition of V_1 (35), we have:

$$\frac{dV_1}{dt} \leq -2DV_1 \leq 0.$$

□

Task 4. Integration of the dV_1/dt expression.

From the above expression, it follows that:

$$V_1 \leq V_{1to}e^{-2D(t-t_o)}. \tag{45}$$

That is, $V_1(35)$ converges exponentially to zero, and consequently f_{v1} converges exponentially to zero. Further, accounting for the definition of f_{v1} (29), it follows that x_1 converges asymptotically to $\Omega_{x1} = \left\{ x_1 : x_1^l \leq x_1 \leq x_1^u \right\}$. From this convergence result and the definition of x_1 (8), it follows that S_1 converges asymptotically to Ω_{S1}; where,

$$\Omega_{S1} = \left[S_1^l \ S_1^u \right], \tag{46}$$

$$S_1^l = x_1^l + S_1^{eq}, \ S_1^u = x_1^u + S_1^{eq}. \tag{47}$$

S_1^{eq} is provided by Equation (5), the bounds x_1^l, x_1^u are defined in Equations (24) and (25). This completes the proof of Ti.

From Equation (44) and properties (31) and (32), it follows that $\frac{dV_1}{dt} < 0 \ for \ x_1 \notin \Omega_{x1}$ and $\frac{dV_1}{dt} \leq 0 \ for \ x_1 \in \Omega_{x1}$. Therefore, the set Ω_{x1} is invariant, and consequently, Ω_{s1} is invariant. This completes the proof of Tii. □

Remark 1. *The property $|g_t| \geq |f_{v1}|$ (42) is crucial for proving the asymptotic convergence of x_1.*

Remark 2. *The invariance of the set Ω_{s1} stated in Theorem 1 implies that once the state S_1 is inside the convergence region Ω_{s1}, that is, $S_1 \in \Omega_{s1}$, it remains inside afterwards.*

3.2. Stability Analysis for the Second and Third Tanks

The stability analysis and majorly the proof for asymptotic convergence of x_2 and x_3 to their compact sets, is based on determining the non-positive nature of $dV/dt = dV_1/dt + k_2 dV_2/dt + k_3 dV_3/dt$, where $V = V_1 + kV_2 + kV_3$, V is the overall Lyapunov function, V_2 is the dead zone quadratic form for the state x_2 and V_3 the dead zone quadratic form for the state x_3, and k_2 and k_3 are positive constants. To achieve this goal, the functions V_2 and V_3 and the gradients dV_2/dx_2 and dV_3/dx_3 are defined accordingly, and the non-positive nature of the terms of the dV/dt expression is determined.

The procedure comprises the following tasks: (i) determination of the expression for $dV_2/dt + kdV_3/dt$; (ii) arrangement of the expression for $dV_2/dt + kdV_3/dt$ in terms of f_{v1}; (iii) definition of gradient dV_2/dx_2 and dead zone quadratic form V_2; (iv) arrangement of

the expression for $dV_2/dt + kdV_3/dt$ in terms of a non-positive function of dV_2/dx_2; (v) definition of gradient dV_3/dx_3 and dead zone quadratic form V_3; (vi) definition of the overall Lyapunov function V and determination of the non-positive nature of the expression for $dV/dt = dV_1/dt + kdV_2/dt + kdV_3/dt$; (vii) integration of the dV/dt expression. The definition of the gradients dV_2/dx_2 and dV_3/dx_3 and the quadratic forms V_2 and V_3 requires the determination of the expression for $dV_2/dt + kdV_3/dt$ and the properties of the terms involved.

Theorem 2. *Consider the model (11)–(15), subject to assumptions 1 to 3. (Ti) the state x_2 converges asymptotically to Ω_{x2}, $\Omega_{x2} = \left\{ x_2 : x_2^l \leq x_2 \leq x_2^u \right\}$, where:*

$$x_2^u = \{x_2 : g_{x2} - max\{\delta_2\} = 0\}, \ x_2^u > 0 x_2^l = \{x_2 : g_{x2} - min\{\delta_2\} = 0\}, \ x_2^l < 0 g_{x2} = x_2 + \tfrac{r_{x2}}{Q/v_2}, \delta_2 = -d_{x1}, d_{x1} = \begin{cases} -x_1^u \ for \ x_1 > x_1^u \\ -x_1 \ for \ x_1 \in \left[x_1^l, \ x_1^u \right] \\ -x_1^l \ for \ x_1 < x_1^l \end{cases}.$$

S_2 converges asymptotically to Ω_{S2} where $\Omega_{S2} = \left[S_2^l \ S_2^u \right]$, $S_2^l = x_2^l + S_2^{eq}$, $S_2^u = x_2^u + S_2^{eq}$ and S_2^{eq} is provided by Equations (5)–(7). (Tii) the state x_3 converges asymptotically to Ω_{x3}, $\Omega_{x3} = \left\{ x_3 : x_3^l \leq x_3 \leq x_3^u \right\}$, where $x_3^u = x_2^u$; $x_3^l = x_2^l$, and S_3 converges asymptotically to Ω_{S3} where $\Omega_{S3} = \left[S_3^l \ S_3^u \right]$, $S_3^l = x_3^l + S_3^{eq}$, $S_3^u = x_3^u + S_3^{eq}$ and S_3^{eq} is provided by Equations (5)–(7). (Tiii) The sets $\Omega_x = \Omega_{x1} \bigcup \Omega_{x2} \bigcup \Omega_{x3}$ and $\Omega_S = \Omega_{S1} \bigcup \Omega_{S2} \bigcup \Omega_{S3}$ are invariant.

Proof. Task 1. Determination of the expression for $dV_2/dt + kdV_3/dt$.

The dx_2/dt expression (13) can be rewritten as:

$$\frac{dx_2}{dt} = -\frac{Q_D}{v_2}(x_2 - x_3) + (-1)\frac{Q}{v_2}(g_{x2} - x_1), \tag{48}$$

where:

$$g_{x2} = x_2 + \frac{r_{x2}}{Q/v_2}. \tag{49}$$

The time derivative of V_2 can be expressed as:

$$\frac{dV_2}{dt} = f_{v2}\frac{dx_2}{dt}, \tag{50}$$

$$f_{v2} = \frac{dV_2}{dx_2}. \tag{51}$$

Substituting the dx_2/dt expression (Equation (48)) and arranging, yields:

$$\frac{dV_2}{dt} = f_{v2}(-1)\frac{Q_D}{v_2}(x_2 - x_3) + (-1)\frac{Q}{v_2}f_{v2}(g_{x2} - x_1). \tag{52}$$

The time derivative of V_3 can be expressed as:

$$\frac{dV_3}{dt} = f_{v3}\frac{dx_3}{dt}, \tag{53}$$

$$f_{v3} = \frac{dV_3}{dx_3}. \tag{54}$$

Substituting the dx_3/dt expression (Equation (15)) and arranging, yields

$$\frac{dV_3}{dt} = f_{v3}\left((x_2 - x_3)\frac{Q_D}{v_3} \right). \tag{55}$$

Hence,

$$\frac{d}{dt}\left(\frac{v_3}{v_2}V_3\right) = f_{v3}\left((x_2 - x_3)\frac{Q_D}{v_2}\right). \tag{56}$$

Adding dV_2/dt (52) and dV_3/dt (56), yields

$$\frac{dV_2}{dt} + \frac{d}{dt}\left(\frac{v_3}{v_2}V_3\right) = (-1)\frac{Q_D}{v_2}(x_2 - x_3)(f_{v2} - f_{v3}) + (-1)\frac{Q}{v_2}f_{v2}(g_{x2} - x_1). \tag{57}$$

□

Task 2. Arrangement of the expression for $dV_2/dt + kdV_3/dt$ in terms of f_{v1}.

The x_1 signal appearing in Equation (57) can be expressed as the sum of f_{v1} and a disturbance term. Let,

$$d_{x1} = f_{v1} - x_1. \tag{58}$$

Using the definition of f_{v1} (29), we have:

$$d_{x1} = \begin{cases} -x_1^u \ for \ x_1 > x_1^u \\ -x_1 \ for \ x_1 \ \in \ \left[x_1^l, x_1^u\right] \\ -x_1^l \ for \ x_1 < x_1^l \end{cases}. \tag{59}$$

Hence,

$$d_{x1} \in \left[-x_1^u, -x_1^l\right]. \tag{60}$$

From Equation (58), x_1 can be expressed as:

$$x_1 = f_{v1} - d_{x1}. \tag{61}$$

Substituting in expression (57) and arranging, yields:

$$\begin{aligned} \frac{dV_2}{dt} + \frac{d}{dt}\left(\frac{v_3}{v_2}V_3\right) &= (-1)\frac{Q_D}{v_2}(x_2 - x_3)(f_{v2} - f_{v3}) + (-1)\frac{Q}{v_2}f_{v2}(g_{x2} - \delta_2) \\ &\quad + f_{v2}\frac{Q}{v_2}f_{v1}. \end{aligned} \tag{62}$$

where

$$\delta_2 = -d_{x_1}. \tag{63}$$

The effect of the term $f_{v2}(Q/v_2)f_{v1}$ is tackled later by considering the dV_1/dt expression. □

Task 3. Definition of gradient $f_{v2} = dV_2/dx_2$ and dead zone quadratic form V_2.

At what follows, we examine the properties of δ_2 and the term $g_{x2} - \delta_2$ appearing in Equation (62), what allows us to choose f_{v2} and V_2. From the definition of δ_2 (63) and d_{x1} (59) it follows that $\delta_2 \in \left[x_1^l, \ x_1^u\right]$.

Hence,

$$max\{\delta_2\} = x_1^u > 0, \tag{64}$$

$$min\{\delta_2\} = x_1^l < 0. \tag{65}$$

The gradient of g_{x2} (49) is:

$$\frac{dg_{x2}}{dx_2} = 1 + \frac{1}{Q/v_2}\frac{d\bar{r}_{x2}}{dx_2}. \tag{66}$$

Furthermore, accounting for the definition of r_{x2} (14), the definition of g_{x2} in Equation (49), and the properties of r_{x2} stated in assumption 3, we have:

$$\frac{dg_{x2}}{dx_2} \geq 1, \ \frac{dg_{x2}}{dx_2} \ is \ bounded \ for \ x_2 \ bounded, \ and \ sgn(g_{x2}) = sgn(x_2). \tag{67}$$

In turn, these properties lead to:

$$g_{x2} - \delta_2 > 0 \quad for \ x_2 > x_2^u > 0, \tag{68}$$

$$g_{x2} - \delta_2 < 0 \quad for \ x_2 < x_2^l < 0. \tag{69}$$

where

$$x_2^u = \{x_2 : \ g_{x2} - max\{\delta_2\} = 0\}, x_2^u > 0, \tag{70}$$

$$x_2^l = \{x_2 : \ g_{x2} - min\{\delta_2\} = 0\}, x_2^l < 0. \tag{71}$$

The term δ_2 is defined in Equations (63) and (59) and satisfies Equations (64) and (65). From Equations (67)–(69) it follows that:

$$sgn(g_{x2} - \delta_2) = sgn(x_2) = sgn(g_{x2}) \ for \ x_2 \notin \left[x_2^l, x_2^u\right]. \tag{72}$$

To obtain the non-positive nature of the term $(-1)f_{v2}(g_{x2} - \delta_2)$, appearing in Equation (62), we need to choose f_{v2} such that:

$$-f_{v2}(g_{x2} - \delta_2) < 0 \ for \ x_2 \notin \left[x_2^l, x_2^u\right], \tag{73}$$

$$-f_{v2}(g_{x2} - \delta_2) = 0 \ for \ x_2 \in \left[x_2^l, x_2^u\right]. \tag{74}$$

In view of properties (72) and to fulfill (73) and (74), we choose:

$$f_{v2} = \begin{cases} x_2 - x_2^u \ for \ x_2 > x_2^u > 0 \\ 0 \ for \ x_2 \in \left[x_2^l, \ x_2^u\right] \\ x_2 - x_2^l \ for \ x_2 < x_2^l < 0 \end{cases}. \tag{75}$$

The main properties of f_{v2} are:

$$(Pi) \ f_{v2} \ is \ continuous \ with \ respect \ to \ x_2, \tag{76}$$

$$(Pii) \ f_{v2} = 0 \ for \ x_2 \in \left[x_2^l, x_2^u\right], \tag{77}$$

$$(Piii) \ f_{v2} \neq 0 \ for \ x_2 \notin \left[x_2^l, \ x_2^u\right], \tag{78}$$

$$(Piv) \ sgn(f_{v2}) = sgn(x_2) \neq 0 \ for \ x_2 \notin \left[x_2^l, x_2^u\right], \tag{79}$$

$$(Pv) \ sgn(f_{v2}) = sgn(g_{x2}) = sgn(g_{x2} - \delta_2) \neq 0 \ for \ x_2 \notin \left[x_2^l, \ x_2^u\right]. \tag{80}$$

A Lyapunov function that satisfies $dV_2/dx_2 = f_{v2}$ Equation (51) is:

$$V_2 = \frac{1}{2}f_{v2}^2. \tag{81}$$

The main properties of V_2 are:

$$V_2 > 0 \ for \ \ x_2 \notin \left[x_2^l, x_2^u\right], \tag{82}$$

$$V_2 = 0 \ for \ x_2 \in \left[x_2^l, x_2^u\right], \tag{83}$$

$$V_2 \ is \ continuous \ with \ respect \ to \ x_2. \tag{84}$$

□

Task 4. Arrangement of the expression for $dV_2/dt + kdV_3/dt$ in terms of a non-positive function of $f_{v2} = dV_2/dx_2$.

From properties Pv (80) and Pii (77), it follows that the term $f_{v2}(g_{x2} - \delta_2)$ appearing in Equation (62) satisfies:

$$f_{v2}(g_{x2} - \delta_2) = |f_{v2}||g_{x2} - \delta_2| = |f_{v2}(g_{x2} - \delta_2)| \geq 0. \tag{85}$$

In addition, the term $(g_{x2} - \delta_2)$ satisfies the following:

$$|g_{x2} - \delta_2| \geq |g_{2v}|, \tag{86}$$

where,

$$g_{2v} = \begin{cases} g_{x2} - max\{\delta_2\} \, for \, x_2 > x_2^u \\ 0 \, for \, x_2 \in \left[x_2^l, \, x_2^u\right] \\ g_{x2} - min\{\delta_2\} \, for \, x_2 < x_2^l \end{cases}. \tag{87}$$

The main properties of g_{2v} are:

$$(Pi) \, g_{2v} \, is \, continuous \, with \, respect \, to \, x_2, \tag{88}$$

$$(Pii) \, g_{2v} = 0 \, for \, x_2 \in \left[x_2^l, \, x_2^u\right], \tag{89}$$

$$(Piii) \, g_{2v} \neq 0 \, for \, x_2 \notin \left[x_2^l, \, x_2^u\right], \tag{90}$$

$$(Piv) \, sgn(g_{2v}) = sgn(x_2) \neq 0 \, for \, x_2 \notin \left[x_2^l, \, x_2^u\right]. \tag{91}$$

From Equations (85) and (86), it follows that:

$$f_{v2}(g_{x2} - \delta_2) = |f_{v2}||g_{x2} - \delta_2| \geq |f_{v2}g_{2v}| \geq 0. \tag{92}$$

From the definitions of g_{2v} (87) and f_{v2} (75) it follows that:

$$|g_{2v}| \geq |f_{v2}|. \tag{93}$$

Therefore, Equation (92) yields:

$$f_{v2}(g_{x2} - \delta_2) \geq f_{v2}^2 \geq 0. \tag{94}$$

Using this, Equation (62), yields:

$$\frac{dV_2}{dt} + \frac{d}{dt}\left(\frac{v_3}{v_2}V_3\right) \leq (-1)\frac{Q_D}{v_2}(x_2 - x_3)(f_{v2} - f_{v3}) + (-1)\frac{Q}{v_2}f_{v2}^2 + f_{v2}\frac{Q}{v_2}f_{v1}. \tag{95}$$

□

Task 5. Definition of gradient dV_3/dx_3 and dead zone quadratic form V_3.

We choose f_{v3} with the structure of f_{v2}:

$$f_{v3} = \begin{cases} x_3 - x_3^u \, for \, x_3 > x_3^u > 0 \\ 0 \, for \, x_3 \in \left[x_3^l, \, x_3^u\right] \\ x_3 - x_3^l \, for \, x_3 < x_3^l < 0 \end{cases}. \tag{96}$$

where the bounds x_3^u, x_3^l are defined as:

$$x_3^u = x_2^u; \, x_3^l = x_2^l, \tag{97}$$

and x_2^l, x_2^u are defined in Equations (70) and (71). A Lyapunov function that satisfies the gradient $dV_3/dx_3 = f_{v3}$ (Equation (54)) is:

$$V_3 = \frac{1}{2} f_{v3}^2 \tag{98}$$

The main properties of V_3 are:

$$V_3 > 0 \; for \;\; x_3 \notin \left[x_3^l, \; x_3^u \right], \tag{99}$$

$$V_3 = 0 \; for \; x_3 \in \left[x_3^l, \; x_3^u \right], \tag{100}$$

$$V_3 \text{ is continuous with respect to } x_3. \tag{101}$$

As a consequence of the definitions of f_{v2} (75) and f_{v3} (96), the property:

$$(x_2 - x_3)(f_{v2} - f_{v3}) \geq 0, \tag{102}$$

holds true, as proved in Appendix A. Equation (95) can be arranged as:

$$\frac{dV_2}{dt} + \frac{d}{dt}\left(\frac{v_3}{v_2}V_3\right) \leq (-1)\frac{Q_D}{v_2}(x_2 - x_3)(f_{v2} - f_{v3}) - \beta_1 \frac{Q}{v_2}f_{v2}^2 + (-1)\beta_2 \frac{Q}{v_2}f_{v2}^2 + f_{v2}\frac{Q}{v_2}f_{v1}, \tag{103}$$

where β_1, β_2 are positive constants that satisfy:

$$1 = \beta_1 + \beta_2, \;\; \beta_1 \in (0, \, 1), \;\; \beta_2 \in (0, \, 1). \tag{104}$$

$\square$

Task 6. Definition of the overall Lyapunov function V and determination of the non-positive nature of the expression for $dV/dt = dV_1/dt + kdV_2/dt + dV_3/dt$.

The term $(-1)\beta_2 \frac{Q}{v_2}f_{v2}^2 + f_{v2}\frac{Q}{v_2}f_{v1}$ appearing in Equation (103) can be expressed in terms of f_{v1}^2:

$$(-1)\beta_2 \frac{Q}{v_2}f_{v2}^2 + f_{v2}\frac{Q}{v_2}f_{v1} = (-1)\beta_2 \frac{Q}{v_2}\left(f_{v2} - \frac{1}{2\beta_2}f_{v1}\right)^2 + \frac{1}{4\beta_2}\frac{Q}{v_2}f_{v1}^2 \leq \frac{1}{4\beta_2}\frac{Q}{v_2}f_{v1}^2. \tag{105}$$

Substituting into Equation (103), we have:

$$\frac{dV_2}{dt} + \frac{d}{dt}\left(\frac{v_3}{v_2}V_3\right) \leq (-1)\frac{Q_D}{v_2}(x_2 - x_3)(f_{v2} - f_{v3}) + (-1)\beta_1 \frac{Q}{v_2}f_{v2}^2 + \frac{1}{4\beta_2}\frac{Q}{v_2}f_{v1}^2. \tag{106}$$

We tackle the effect of the f_{v1}^2 term by incorporating the dV_1/dt expression. Equation (44) leads to:

$$\frac{d}{dt}\left(\frac{1}{D}\frac{1}{4\beta_2}\frac{Q}{v_2}V_1\right) \leq -\frac{1}{4\beta_2}\frac{Q}{v_2}f_{v1}^2. \tag{107}$$

Combining with Equation (106) and accounting for the property (102), yields:

$$\frac{dV_2}{dt} + \frac{d}{dt}\left(\frac{v_3}{v_2}V_3\right) + \frac{d}{dt}\left(\frac{1}{D}\frac{1}{4\beta_2}\frac{Q}{v_2}V_1\right) \leq (-1)\frac{Q_D}{v_2}(x_2 - x_3)(f_{v2} - f_{v3}) + (-1)\beta_1 \frac{Q}{v_2}f_{v2}^2 \leq 0, \tag{108}$$

which can be rewritten as:

$$\frac{dV}{dt} \leq (-1)\frac{Q_D}{v_2}(x_2 - x_3)(f_{v2} - f_{v3}) + (-1)\beta_1 \frac{Q}{v_2}f_{v2}^2 \leq 0. \tag{109}$$

where V is the overall Lyapunov function, defined as:

$$V = V_2 + \frac{v_3}{v_2}V_3 + \frac{1}{D}\frac{1}{4\beta_2}\frac{Q}{v_2}V_1. \tag{110}$$

□

Task 7. Integration of the dV/dt expression.

Integrating Equation (108), yields:

$$V_2 + \frac{v_3}{v_2}V_3 + \frac{1}{4\beta_2}\frac{1}{D}\frac{Q}{v_2}V_1 + \beta_1\frac{Q}{v_2}\int_{to}^{t}f_{v2}^2 dt + \int_{to}^{t}\frac{Q_D}{v_2}(x_2 - x_3)(f_{v2} - f_{v3})dt \leq V_{2to} + \frac{v_3}{v_2}V_{3to} + \frac{1}{4\beta_2}\frac{1}{D}\frac{Q}{v_2}V_{1to}. \tag{111}$$

Therefore: (BPi) $V_2 \in \mathcal{L}_\infty$, $V_3 \in \mathcal{L}_\infty$, $V_1 \in \mathcal{L}_\infty$, and from the definitions of V_1 (35), V_2 (81), V_3 (98) it follows that $f_{v1} \in \mathcal{L}_\infty$, $f_{v2} \in \mathcal{L}_\infty$, $f_{v3} \in \mathcal{L}_\infty$, and consequently $f_{v2}^2 \in \mathcal{L}_\infty$; (BPii) $x_1 \in \mathcal{L}_\infty$, $x_2 \in \mathcal{L}_\infty$, $x_3 \in \mathcal{L}_\infty$, what follows from the definitions of f_{v1} (29), f_{v2} (75), f_{v3} (96); (BPiii) $f_{v2}^2 \in \mathcal{L}_1$. Considering the properties $f_{v2}^2 \in \mathcal{L}_1$ and $f_{v2}^2 \in \mathcal{L}_\infty$ and applying the Barbalat's lemma (cf. [36]), yields:

$$\lim_{t\to\infty}f_{v2}^2 = 0. \tag{112}$$

Furthermore, accounting for the definition of f_{v2} (75), it follows that x_2 converges asymptotically to $\Omega_{x2} = \left\{x_2 : x_2^l \leq x_2 \leq x_2^u\right\}$. From this convergence result and the definition of x_2 (9), it follows that S_2 converges asymptotically to Ω_{S2}; where:

$$\Omega_{S2} = \begin{bmatrix} S_2^l & S_2^u \end{bmatrix}, \tag{113}$$

$$S_2^l = x_2^l + S_2^{eq}, \ S_2^u = x_2^u + S_2^{eq}. \tag{114}$$

S_2^{eq} is provided by Equations (5)–(7); the bounds x_2^l, x_2^u are defined in Equations (70) and (71). This completes the proof of the first part of the theorem (Ti).

From Equation (111), it follows that $(x_2 - x_3)(f_{v2} - f_{v3}) \in L_1$ and from properties Bpi, BPii it follows that $(x_2 - x_3)(f_{v2} - f_{v3}) \in L_\infty$. Applying the Lasalle's theorem (cf. [22]) yields $\lim_{t\to\infty}(x_2 - x_3)(f_{v2} - f_{v3}) = 0$.

Hence, either $x_2 - x_3$ or $f_{v2} - f_{v3}$ converges to zero. This result and the convergence of x_2 to Ω_{x2}, the convergence of f_{v2} to zero, and the definition of f_{v3} (96) and f_{v2} (75), imply: (i) if $x_2 - x_3$ converges to zero, then x_3 converges to Ω_{x3}, $\Omega_{x3} = \left\{x_3 : x_3^l \leq x_3 \leq x_3^u\right\}$; (ii) if $f_{v2} - f_{v3}$ converges to zero, then f_{v3} converges to zero, which implies the convergence of x_3 to Ω_{x3}. Therefore, as is indicated by both of these possibilities, x_3 converges asymptotically to Ω_{x3}. From this convergence result and the definition of x_3 (10) it follows that S_3 converges asymptotically to Ω_{S3}, where:

$$\Omega_{S3} = \begin{bmatrix} S_3^l S_3^u \end{bmatrix}, \tag{115}$$

$$S_3^l = x_3^l + S_3^{eq}, \ S_3^u = x_3^u + S_3^{eq}. \tag{116}$$

S_3^{eq} is provided by Equations (5)–(7), and the bounds x_3^l, x_3^u are defined in Equation (97). This completes the proof of the second part of the theorem (Tii).

From Equation (109), it follows that:

$$if \ V = 0 \ for \ t = t^*, \quad t^* \geq t_o, \quad then \ V = 0 \ for \ t \geq t^*. \tag{117}$$

The condition $V = 0$ implies: (i) $f_{v1} = 0$, $f_{v2} = 0$ and $f_{v3} = 0$, as follows from definitions of V (110), V_1 (35), V_2 (81), and V_3 (98); (ii) $x_1 \in \Omega_{x1}$, $x_2 \in \Omega_{x2}$, $x_3 \in \Omega_{x3}$, as follows from the definition of f_{v1} (29), f_{v2} (75) and f_{v3} (96). Therefore, it follows from (117) that $\Omega_x = \Omega_{x1} \bigcup \Omega_{x2} \bigcup \Omega_{x3}$ is invariant, and consequently $\Omega_s = \Omega_{s1} \bigcup \Omega_{s2} \bigcup \Omega_{s3}$ is invariant. This completes the proof of Tiii. □

Remark 1. *Important advantages of the stability result stated in theorem 2 are:*

- *the widths of the convergence regions Ω_{x1}, Ω_{x2}, Ω_{x3} are arbitrarily large, as they are a function of δ_{si}, which is arbitrarily large but bounded;*
- *the initial values of x_1, x_2, and x_3 can take arbitrarily large but bounded positive values, since x_1 is defined in $[-S_1^{eq}, \infty)$, x_2 is defined in $[-S_2^{eq}, \infty)$, and x_3 is defined in $[-S_3^{eq}, \infty)$, as stated in Section 2.*

Remark 2. *In the study of the stability of x_1, the dynamics of x_2 and x_3 (2), (3) are not accounted for, as can be noticed in the proof of Theorem 1. This is a consequence of the fact that x_2 and x_3 are not involved in the dynamics of x_1 (11). In contrast, in the study of the stability of x_2 and x_3, the dynamics of x_1, x_2 and x_3 are accounted for, as can be noticed in the proof of theorem 2. This is a consequence of the fact that x_1, x_2 and x_3 are involved in the dynamics of x_2 (13).*

Remark 3. *The first tank influences the transient value of x_2, which can be noticed from Equation (111). Also, the first tank influences the width of the convergence region of x_2, that is $[x_2^l, x_2^u]$, what can be noticed from the definition of x_2^l, x_2^u (70), (71), the definition of δ_2 (63), (58), the properties of δ_2 (64), (65), and the definition of x_1^l, x_1^u(24), (25).*

Remark 4. *The presence of the third tank influences the transient value of x_2, what can be noticed from Equation (111). However, it does not influence the width of the convergence region of the state x_2, that is, $[x_2^l, x_2^u]$, since the bounds (x_2^l, x_2^u) are not influenced by the parameters of the third tank, that is, Q_D and v_3, which can be noticed from the definition of x_2^l, x_2^u (70), (71).*

Remark 5. *Important tasks of the stability analysis are: the definition of the overall Lyapunov-like function V (110) consisting on the weighted sum of three dead-zoned quadratic forms; the determination of the property (102), which expresses the effect of the flow exchange on the non-positive nature of dV/dt; the property $|g_{2v}| \geq |f_{2v}|$ (93) which was required for proving the convergence of x_2. These tasks are crucial for proving the non-positive nature of dV/dt. Also, the whole stability analysis and especially these tasks are major contributions to the study of convergence of biological processes to compact sets.*

Remark 6. *The invariance of the set Ω_s stated in Theorem 2 implies that once the three states S_1, S_2, S_3 are inside the convergence region Ω_s, that is, $S_1 \in \Omega_{s1}$, $S_2 \in \Omega_{s2}$ and $S_3 \in \Omega_{s3}$ simultaneously, they remain inside afterwards.*

Remark 7. *The developed stability analysis can be extended to other types of nonlinear connected systems, featuring a higher number of state variables, and a vector field with different non-linear terms, by using the following general procedure: (i) determination of the equilibrium points corresponding to the case of no time varying external disturbance; (ii) definition of the new states as the differences between the current state variables and their equilibria; (iii) rewriting of the system dynamics in terms of the new states; (iv) definition of the subsystem Lyapunov functions, corresponding to each state variable, and determination of its properties; (v) determination of the time derivative of each subsystem Lyapunov function, arrangement in terms of non-positive functions and definition of the convergence regions; (vi) definition of the overall Lyapunov function V as a weighted sum of the subsystem Lyapunov functions; (vii) determination of the dV/dt expression and arrangement in terms of non-positive functions; (viii) integration of the dV/dt expression, determination of the boundedness properties of the state variables and their functions; (ix) application of the Barbalat's lemma. As part of this procedure: the subsystem Lyapunov functions can be defined as dead-zone quadratic forms, or they can be defined according to the non-linear terms of the vector field; the subsystem Lyapunov functions corresponding to the state variables featuring connection must be chosen so as to obtain a non-positive effect in the dV/dt expression; if there are one or more state variables whose vector field is independent of the other states, an independent stability analysis can be performed for each of them.*

4. Simulation and Analysis

In this section, some simulations of the system (1)–(3) are performed to illustrate the results stated in Theorems 1 and 2.

We consider the following reaction rate expressions:

$$r_{s1} = \mu_{mx1} \frac{S_1}{K_1 + S_1}, \text{ hence } r_{s1} = \mu_{mx1} \frac{x_1 + S_1^{eq}}{K_1 + x_1 + S_1^{eq}}, r_{s2} = \mu_{mx2} \frac{S_2}{K_2 + S_2}, \text{ hence } r_{s2} = \mu_{mx2} \frac{x_2 + S_2^{eq}}{K_2 + x_2 + S_2^{eq}}.$$

The terms r_{s1} and r_{s2} satisfy assumption 3. The model (1)–(3) with these reaction rate expressions was calibrated with data of suspended solids concentration from vertical subsurface flow constructed wetlands (CWs) reported in [37]. The CWs are located in Cuenca (Ecuador) and receive domestic wastewater coming out from primary treatment. The influent wastewater comprises a suspended solids concentration of 88.83 mg/L, BOD_5 concentration of 95.75 mg/L, and temperature of 24.6 °C. The hydraulic loading rate (HLR) is 0.2 md^{-1}.

Model (1)–(3) was fitted by minimizing the sum of the square residuals between experimental and model data of suspended solids concentration. The parameter values obtained were used in the first simulation case and are shown in Table 1.

Table 1. Parameter values for the CSTR network model (1)–(3).

Parameter	Value for the First Simulation Case	Value for the Second Simulation Case	Value for the Third Simulation Case
Q_1/v_1	0.702 day^{-1}	0.702 day^{-1}	0.702 day^{-1}
Q_2/v_2	0.702 day^{-1}	0.702 day^{-1}	0.702 day^{-1}
Q_D/v_2	0.0001 day^{-1}	0.0001 day^{-1}	0.0001 day^{-1}
Q_D/v_3	1 day^{-1}	1 day^{-1}	1 day^{-1}
μ_{max1}	101 mg /(L day)	101 mg /(L day)	101 mg /(L day)
K_1	303.1 mg/L	303.1 mg/L	303.1 mg/L
μ_{max2}	101 mg/(L day)	202 mg/(L day)	404 mg/(L day)
K_2	303.1 mg/L	151.55 mg/L	30.31 mg/L

To evaluate the obtained convergence results stated in Theorems 1 and 2, model (1)–(4) is simulated with

$$\overline{S}_{in} = 100 \text{ mg/L}; \ \delta_{sin} = A_1 sin\left(\frac{2\pi t}{T_{sin}}\right), \ A_1 = 10; \ T_{sin} = 20 \text{ days.} \tag{118}$$

The bounds S_1^l, S_1^u of Ω_{S1} (47); the bounds S_2^l, S_2^u of Ω_{S2} (114); and the bounds S_3^l, S_3^u of Ω_{S3} (116) are computed and represented by the upper and lower horizontal dotted lines, whereas the equilibrium values S_1^{eq}, S_2^{eq} and S_3^{eq} (Equations (5)–(7)) are represented by the middle horizontal dotted lines. The calculation of the aforementioned bounds requires the calculation of bounds x_1^l, x_1^u (24), (25); x_2^l, x_2^u (70), (71); and x_3^l, x_3^u (97). Three simulations are performed, using definitions (118) and parameter values shown in Table 1.

In the three simulations, convergence to the regions within the calculated bounds is observed: the state S_1 convergences to the region within computed bounds S_1^l, S_1^u (see Figure 2a, Figure 3a, Figure 4a,b); the state S_2 converges to the region within computed bounds S_2^l, S_2^u (see Figure 2b, Figure 3b, Figure 4c,d); and S_3 converges to the region within the computed bounds S_3^l, S_3^u (see Figure 2b, Figure 3b, Figure 4c,d).
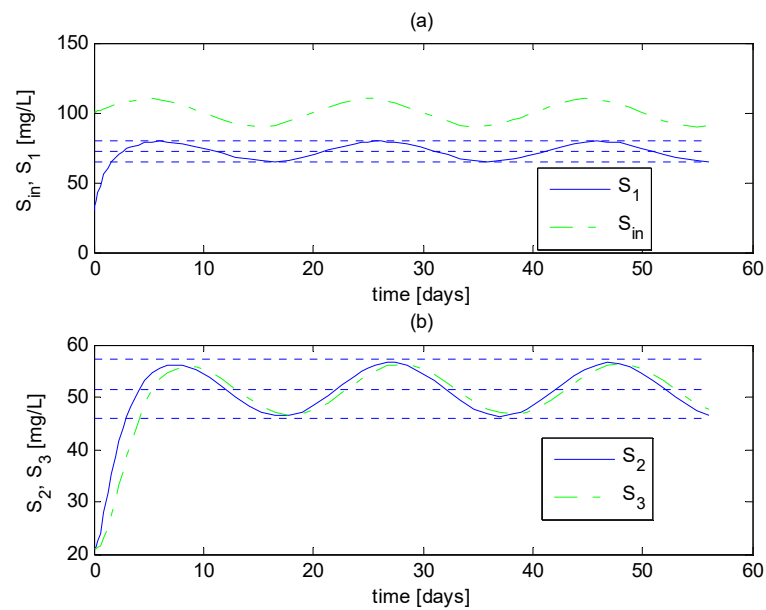
Figure 2. Simulation of the CSTR network model (1)–(4), first case. (**a**) Time course of S_1; the upper and lower horizontal dotted lines indicate the bounds of Ω_{S1}. (**b**) Time course of S_2 and S_3, the upper and lower horizontal dotted lines indicate the bounds of Ω_{S2}, and Ω_{S3}.
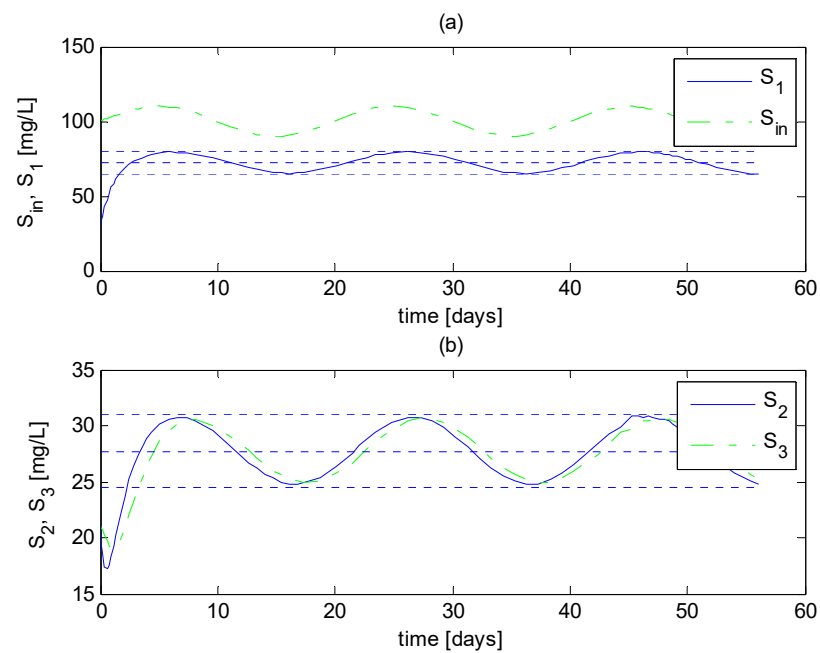
Figure 3. Simulation of the CSTR network model (1)–(4), second case. (**a**) Time course of S_1; the upper and lower horizontal dotted lines indicate the bounds of Ω_{S1}. (**b**) Time course of S_2 and S_3, the upper and lower horizontal dotted lines indicate the bounds of Ω_{S2} and Ω_{S3}.
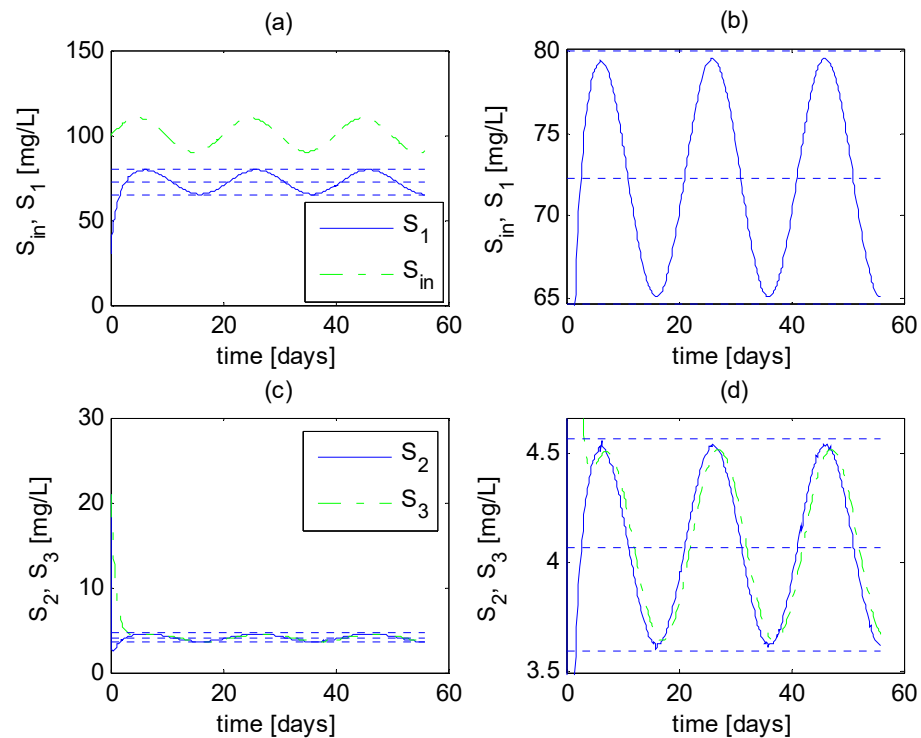
Figure 4. Simulation of the CSTR network model (1)–(4), third case. (**a**) Time course of S_1; the upper and lower horizontal dotted lines indicate the bounds of Ω_{S1}. (**b**) Detail of the time course of S_1. (**c**) Time course of S_2 and S_3, the upper and lower horizontal dotted lines indicate the bounds of Ω_{S2} and Ω_{S3}. (**d**) Detail of the time course of S_2 and S_3.

Also, the three simulation cases illustrate the results stated in Theorems 1 and 2: (i) the invariant nature of Ω_{s1}, stated in Theorem 1 and discussed in Remark 2: one can see that once S_1 enters Ω_{s1}, it remains inside; (ii) the equivalence of the convergence regions Ω_{s2} and Ω_{s3} defined in Theorem 2: one can see that S_2 and S_3 converge to the same regions; (iii) the definitions of Ω_{s1} and Ω_{s2}, which indicate that Ω_{s1} and Ω_{s2} can be quite different, as Ω_{s2} depends on the reaction rate r_{x2}: one can see this remarkable difference in the regions to which S_1 and S_2 converge; (iv) the invariant nature of Ω_s, stated in Theorem 2 and discussed in Remark 6: one can see that once the three state variables are inside the convergence region Ω_s, that is, $S_1 \in \Omega_{s1}$, $S_2 \in \Omega_{s2}$, $S_3 \in \Omega_{s3}$, simultaneously, they remain inside afterwards.

5. Conclusions

This paper presented the analysis of the stability of a network model comprising three CSTRs with the following features: (i) the pollutant concentration in the inflow of the first CSTR is time varying but bounded; (ii) the first and second CSTRs are connected in series, whereas the second and third CSTRs are connected in parallel with flow exchange; (iii) the states converge to a compact set instead of an equilibrium point. The practical applicability of the arrangement of CSTRs is the creation of a simpler model of pollution removal from wastewater treatment via constructed wetlands, generating a satisfactory description of experimental pollution values with a satisfactory transport dead time.

The convergence sets of the states of the CSTR model were determined, and the global asymptotic convergence to these compact sets and their invariance were proved. Also, the effect of the side tank (third tank) on the transient value of the system states was determined, and it was concluded that it had no effect on the convergence regions. To this end, the proposed stability analysis comprises:

(i)   the definition of a dead-zone Lyapunov-like function for each state, the determination of its properties, and the definition of the overall Lyapunov function as the sum of the dead zone quadratic forms;

(ii)   the determination of the time derivative of the quadratic forms and their properties;

(iii) the use of these properties in the time derivative of the overall Lyapunov-like function.

Appendix A

The expression $(x_2 - x_3)(f_{v2} - f_{v3})$ can be expressed as:

$$(x_2 - x_3)(f_{v2} - f_{v3}) = |(x_2 - x_3)(f_{v2} - f_{v3})|\, sgn(x_2 - x_3)\, sgn(f_{v2} - f_{v3}), \tag{A1}$$

or

$$(x_2 - x_3)(f_{v2} - f_{v3}) == |(x_2 - x_3)(f_{v2} - f_{v3})|\, sgn(x_3 - x_2)\, sgn(f_{v3} - f_{v2}). \tag{A2}$$

Thus, the signum of $(x_2 - x_3)(f_{v2} - f_{v3})$ depends on the value of $sgn(x_2 - x_3)$ $sgn(f_{v2} - f_{v3})$, or, equivalently, the signum of $sgn(x_3 - x_2)\, sgn(f_{v3} - f_{v2})$. To determine it, three different cases are analyzed as follows.

Case 1. $|f_{v2}| \neq 0$, $|f_{v3}| \neq 0$. In this case,

$$f_{v2} \neq 0, f_{v3} \neq 0. \tag{A3}$$

From the definitions of f_{v2} (75) and f_{v3} (96) it follows that:

$$x_2 \notin \left[x_2^l, x_2^u\right], x_3 \notin \left[x_3^l, x_3^u\right]. \tag{A4}$$

Hence,

$$sgn(f_{v2}) = sgn(x_2) \neq 0, \tag{A5}$$

$$sgn(f_{v3}) = sgn(x_3) \neq 0. \tag{A6}$$

Therefore, accounting for the definition of f_{v2} and f_{v3}, we have:

$$sgn(f_{v2} - f_{v3}) = sgn(x_2 - x_3). \tag{A7}$$

Therefore, from Equation (A1), it follows that:

$$(x_2 - x_3)(f_{v2} - f_{v3}) \geq 0. \tag{A8}$$

Case 2. $f_{v2} = 0$, $f_{v3} \neq 0$. In this case,

$$x_2 \in \left[x_2^l,\ x_2^u \right], x_3 \notin \left[x_3^l,\ x_3^u \right]. \tag{A9}$$

Moreover,

$$sgn(f_{v2}) = 0, \tag{A10}$$

$$sgn(f_{v3}) = sgn(x_3) \neq 0, \tag{A11}$$

$$sgn(x_3 - x_2) = sgn(x_3) \neq 0. \tag{A12}$$

Furthermore, accounting for the definition of f_{v2} (75) and f_{v3} (96), we have:

$$sgn(f_{v3} - f_{v2}) = sgn(f_{v3}) = sgn(x_3) \neq 0. \tag{A13}$$

Therefore,

$$sgn(f_{v3} - f_{v2})sgn(x_3 - x_2) = +1. \tag{A14}$$

Therefore, from Equation (A2), it follows that:

$$(x_2 - x_3)(f_{v2} - f_{v3}) \geq 0. \tag{A15}$$

Case 3. $f_{v2} \neq 0$, $f_{v3} = 0$. In this case, with a procedure similar to that used for case 2, it is found that:

$$(x_2 - x_3)(f_{v2} - f_{v3}) \geq 0 \tag{A16}$$

References

1. Zhou, G.; Liao, X.; Xu, B.; Yu, P.; Chen, G. Simple algebraic necessary and sufficient conditions for Lyapunov stability of a Chen system and their applications. *Trans. Inst. Meas. Control* **2018**, *40*, 2200–2210. [CrossRef]
2. Liao, X.; Zhou, G.; Yang, Q.; Fu, Y.; Chen, G. Constructive proof of Lagrange stability and sufficient—Necessary conditions of Lyapunov stability for Yang–Chen chaotic system. *Appl. Math. Comput.* **2017**, *309*, 205–221. [CrossRef]
3. Zhang, F.; Liao, X.; Zhang, G.; Mu, C. Dynamical Analysis of the Generalized Lorenz Systems. *J. Dyn. Control Syst.* **2017**, *23*, 349–362. [CrossRef]
4. Meng, R.; Chen, S.; Hua, C.; Qian, J.; Sun, J. Disturbance observer-based output feedback control for uncertain QUAVs with input saturation. *Neurocomputing* **2020**, *413*, 96–106. [CrossRef]
5. Boulkroune, A.; M'saad, M.; Farza, M. Adaptive fuzzy system-based variable-structure controller for multivariable nonaffine nonlinear uncertain systems subject to actuator nonlinearities. *Neural Comput. Appl.* **2017**, *28*, 3371–3384. [CrossRef]
6. Zhang, L.; Wang, Z.; Li, S.; Ding, S.; Du, H. Universal finite-time observer based second-order sliding mode control for DC-DC buck converters with only output voltage measurement. *J. Franklin Inst.* **2020**, *357*, 11863–11879. [CrossRef]
7. Shao, X.; Wang, L.; Li, J.; Liu, J. High-order ESO based output feedback dynamic surface control for quadrotors under position constraints and uncertainties. *Aerosp. Sci. Technol.* **2019**, *89*, 288–298. [CrossRef]
8. Askari, M.R.; Shahrokhi, M.; Khajeh Talkhoncheh, M. Observer-based adaptive fuzzy controller for nonlinear systems with unknown control directions and input saturation. *Fuzzy Sets Syst.* **2017**, *314*, 24–45. [CrossRef]
9. Gao, S.; Ning, B.; Dong, H. Fuzzy dynamic surface control for uncertain nonlinear systems under input saturation via truncated adaptation approach. *Fuzzy Sets Syst.* **2016**, *290*, 100–117. [CrossRef]
10. Min, H.; Xu, S.; Ma, Q.; Zhang, B.; Zhang, Z. Composite-Observer-Based Output-Feedback Control for Nonlinear Time-Delay Systems With Input Saturation and Its Application. *IEEE Trans. Ind. Electron.* **2018**, *65*, 5856–5863. [CrossRef]
11. Zhang, F.; Liao, X.; Zhang, G. On the global boundedness of the Lü system. *Appl. Math. Comput.* **2016**, *284*, 332–339. [CrossRef]
12. Slotine, J.-J.E.; Li, W. *Applied Nonlinear Control*; Prentice Hall: Englewood Cliffs, NJ, USA, 1991; ISBN 0130408905.
13. Koo, K.-M. Stable adaptive fuzzy controller with time-varying dead-zone. *Fuzzy Sets Syst.* **2001**, *121*, 161–168. [CrossRef]
14. Wang, X.-S.; Su, C.-Y.; Hong, H. Robust adaptive control of a class of nonlinear systems with unknown dead-zone. *Automatica* **2004**, *40*, 407–413. [CrossRef]
15. Su, C.-Y.; Feng, Y.; Hong, H.; Chen, X. Adaptive control of system involving complex hysteretic nonlinearities: A generalised Prandtl–Ishlinskii modelling approach. *Int. J. Control* **2009**, *82*, 1786–1793. [CrossRef]
16. Ranjbar, E.; Yaghubi, M.; Abolfazl Suratgar, A. Robust adaptive sliding mode control of a MEMS tunable capacitor based on dead-zone method. *Automatika* **2020**, *61*, 587–601. [CrossRef]
17. Rincón, A.; Hoyos, F.E.; Candelo-Becerra, J.E. Adaptive Control for a Biological Process under Input Saturation and Unknown Control Gain via Dead Zone Lyapunov Functions. *Appl. Sci.* **2021**, *11*, 251. [CrossRef]

18. Rincón, A.; Piarpuzán, D.; Angulo, F. A new adaptive controller for bio-reactors with unknown kinetics and biomass concentration: Guarantees for the boundedness and convergence properties. *Math. Comput. Simul.* **2015**, *112*, 1–13. [CrossRef]

19. Rincón, A.; Florez, G.Y.; Olivar, G. Convergence Assessment of the Trajectories of a Bioreaction System by Using Asymmetric Truncated Vertex Functions. *Symmetry* **2020**, *12*, 513. [CrossRef]

20. Meadows, T.; Weedermann, M.; Wolkowicz, G.S.K. Global Analysis of a Simplified Model of Anaerobic Digestion and a New Result for the Chemostat. *SIAM J. Appl. Math.* **2019**, *79*, 668–689. [CrossRef]

21. Mairet, F.; Ramírez, C.H.; Rojas-Palma, A. Modeling and stability analysis of a microalgal pond with nitrification. *Appl. Math. Model.* **2017**, *51*, 448–468. [CrossRef]

22. Sari, T.; Mazenc, F. Global dynamics of the chemostat with different removal rates and variable yields. *Math. Biosci. Eng.* **2011**, *8*, 827–840. [CrossRef] [PubMed]

23. Almeida, R.; Hristova, S.; Dashkovskiy, S. Uniform bounded input bounded output stability of fractional-order delay nonlinear systems with input. *Int. J. Robust Nonlinear Control* **2021**, *31*, 225–249. [CrossRef]

24. Garrido, H.; Curadelli, O.; Ambrosini, D. On the assumed inherent stability of semi-active control systems. *Eng. Struct.* **2018**, *159*, 286–298. [CrossRef]

25. Vafamand, N.; Asemani, M.H.; Khayatian, A. Robust L1 Observer-Based Non-PDC Controller Design for Persistent Bounded Disturbed TS Fuzzy Systems. *IEEE Trans. Fuzzy Syst.* **2018**, *26*, 1401–1413. [CrossRef]

26. Kong, L.; He, W.; Dong, Y.; Cheng, L.; Yang, C.; Li, Z. Asymmetric Bounded Neural Control for an Uncertain Robot by State Feedback and Output Feedback. *IEEE Trans. Syst. Man Cybern. Syst.* **2019**, 1–12. [CrossRef]

27. Yu, J.; Zhao, L.; Yu, H.; Lin, C. Barrier Lyapunov functions-based command filtered output feedback control for full-state constrained nonlinear systems. *Automatica* **2019**, *105*, 71–79. [CrossRef]

28. Niu, B.; Liu, Y.; Zhou, W.; Li, H.; Duan, P.; Li, J. Multiple Lyapunov Functions for Adaptive Neural Tracking Control of Switched Nonlinear Nonlower-Triangular Systems. *IEEE Trans. Cybern.* **2020**, *50*, 1877–1886. [CrossRef] [PubMed]

29. De Battista, H.; Jamilis, M.; Garelli, F.; Picó, J. Global stabilisation of continuous bioreactors: Tools for analysis and design of feeding laws. *Automatica* **2018**, *89*, 340–348. [CrossRef]

30. El Hajji, M.; Chorfi, N.; Jleli, M. Mathematical modeling and analysis for a three-tiered microbial food web in a chemostat. *Electron. J. Differ. Equ.* **2017**, *2017*, 1–13.

31. Marsili-Libelli, S.; Checchi, N. Identification of dynamic models for horizontal subsurface constructed wetlands. *Ecol. Modell.* **2005**, *187*, 201–218. [CrossRef]

32. Langergraber, G. Applying Process-Based Models for Subsurface Flow Treatment Wetlands: Recent Developments and Challenges. *Water* **2016**, *9*, 5. [CrossRef]

33. Defo, C.; Kaur, R.; Bharadwaj, A.; Lal, K.; Kumar, P. Modelling approaches for simulating wetland pollutant dynamics. *Crit. Rev. Environ. Sci. Technol.* **2017**, *47*, 1371–1408. [CrossRef]

34. Davies, L.C.; Vacas, A.; Novais, J.M.; Freire, F.G.; Martins-Dias, S. Vertical flow constructed wetland for textile effluent treatment. *Water Sci. Technol.* **2007**, *55*, 127–134. [CrossRef] [PubMed]

35. Freire, F.G.; Davies, L.C.; Vacas, A.M.; Novais, J.M.; Martins-Dias, S. Influence of operating conditions on the degradation kinetics of an azo-dye in a vertical flow constructed wetland using a simple mechanistic model. *Ecol. Eng.* **2009**, *35*, 1379–1386. [CrossRef]

36. Ioannou, P.A.; Sun, J. *Robust Adaptive Control*; Prentice Hall: Upper Saddle River, NJ, USA, 1996; ISBN 9780486498171.

37. García-Ávila, F.; Patiño-Chávez, J.; Zhinín-Chimbo, F.; Donoso-Moscoso, S.; Flores del Pino, L.; Avilés-Añazco, A. Performance of Phragmites Australis and Cyperus Papyrus in the treatment of municipal wastewater by vertical flow subsurface constructed wetlands. *Int. Soil Water Conserv. Res.* **2019**, *7*, 286–296. [CrossRef]